kit (Qiagen). Then, 1 μl of the PCR product was used for direct sequencing (ABI PRISM Model 3100, version 3.7, Applied Biosystems). Next, the resulting immunoglobulin sequence was fed into BLAST (NCBI) to identify the closest germline sequences.

Western Blotting

CD27 protein expression in tumor samples was determined by western blot analysis. Protein lysates were analyzed using standard techniques and the anti-CD27 rabbit polyclonal antibody (Abcam, Tokyo, Japan) as described.[13] We included one fresh-frozen reactive lymphoid hyperplasia sample as a positive control, a HeLa cell line sample as a negative control, and three fresh-frozen duodenal FL samples in each analysis.

Statistical Analysis

All statistical analyses were performed with the Mann–Whitney *U*-test using SPSS software (version 14.0; SPSS, Chicago, IL, USA). Values of $P<0.05$ were considered statistically significant.

Results

Clinicopathological Findings

Clinical features (age, gender, and clinical stage), histological grading, and immunohistochemical findings are summarized in Table 1. The study group comprised 16 men and 14 women, aged between 40 and 81 years, with a median age of 61 years (Stomach FL: age range, 51–81 years; median age, 63 years. Duodenum FL: age range, 49–75 years; median age, 61 years. Colon and rectum FL: age range, 40–87 years, median age, 58 years). Clinical stages were determined according to the criteria recommended by the International Workshop (Lugano) and are detailed in Table 1. All stage IV patients had bone marrow involvement. We excluded patients with multiple lymph node lesions. In our patient series, the stage IV patients had both gastrointestinal lesions and bone marrow lesions, and they had predominant gastrointestinal involvement. Typical histological appearance of patient samples showed a vague nodular pattern composed of small- to medium-sized cleaved lymphoid cells. The main locations of gastric and colonic FLs were the submucosal to subserosal areas (Figures 1a–f). Duodenal FLs were located in the submucosal area (Figures 1g–i), and tumor cells were associated with duodenal villi. Histological grades were distributed as follows: grade 1: 24 samples; grade 2: 5 samples; Grade 3A: 1 sample.

Immunophenotyping Results

CD21 expression patterns are shown in Table 2. FDC were arranged at the periphery of tumor follicles in

Table 1 Clinicopathological features in gastrointestinal FLs

Patient no.	*Sites*	*Age (years)/gender*	*Stage*	*Grade*	*CD20*	*CD10*	*CD5*	*Cyclin D1*	*BCL-2*	*BCL-6*	*MUM-1*	*Blimp-1*
1	Stomach	60/M	I	1	+	+	−	−	+	+	−	−
2	Stomach	75/M	IV	1	+	+	−	−	+	+	−	−
3	Stomach	63/M	I	1	+	+	−	−	+	+	−	−
4	Stomach	60/F	I	2	+	+	−	−	+	+	−	−
5	Stomach	51/F	II2	1	+	+	−	−	+	+	−	−
6	Stomach	81/F	I	2	+	+	−	−	+	+	−	−
7	Stomach	51/F	I	2	+	+	−	−	±	+	−	−
8	Stomach	74/M	II1	1	+	+	−	−	+	+	−	−
9	Duodenum	75/M	I	1	+	+	−	−	+	+	−	−
10	Duodenum	57/M	I	1	+	+	−	−	+	+	−	−
11	Duodenum	58/M	IV	1	+	+	−	−	+	+	−	−
12	Duodenum	75/M	II2	1	+	+	−	−	+	+	−	−
13	Duodenum	71/F	I	1	+	+	−	−	+	+	−	−
14	Duodenum	66/F	I	1	+	+	−	−	+	+	−	−
15	Duodenum	51/M	I	1	+	+	−	−	+	+	−	−
16	Duodenum	49/M	II2	1	+	+	−	−	+	+	−	−
17	Duodenum	62/F	II2	1	+	+	−	−	+	+	−	−
18	Duodenum	54/M	I	1	+	+	−	−	+	+	−	−
19	Duodenum	61/F	IV	1	+	+	−	−	+	+	−	−
20	Duodenum	53/F	II2	1	+	+	−	−	+	+	−	−
21	Duodenum	57/F	I	2	+	+	−	−	+	+	−	−
22	Duodenum	56/M	II2	1	+	+	−	−	+	+	−	−
23	Duodenum	66/F	II2	1	+	+	−	−	+	+	−	−
24	Duodenum	55/F	II2	1	+	+	−	−	+	+	−	−
25	Duodenum	63/F	II2	1	+	+	−	−	+	+	−	−
26	Cecum	42/M	II2	2	+	+	−	−	+	+	−	−
27	Colon	40/M	I	1	+	+	−	−	+	+	−	−
28	Colon	47/M	I	3A	+	+	−	−	+	+	−	−
29	Rectum	67/F	I	1	+	+	−	−	+	+	−	−
30	Rectum	77/M	I	1	+	+	−	−	+	+	−	−

Abbreviations: BCL-2, B-cell lymphoma 2; F, female; FL, follicular lymphoma; M, male.

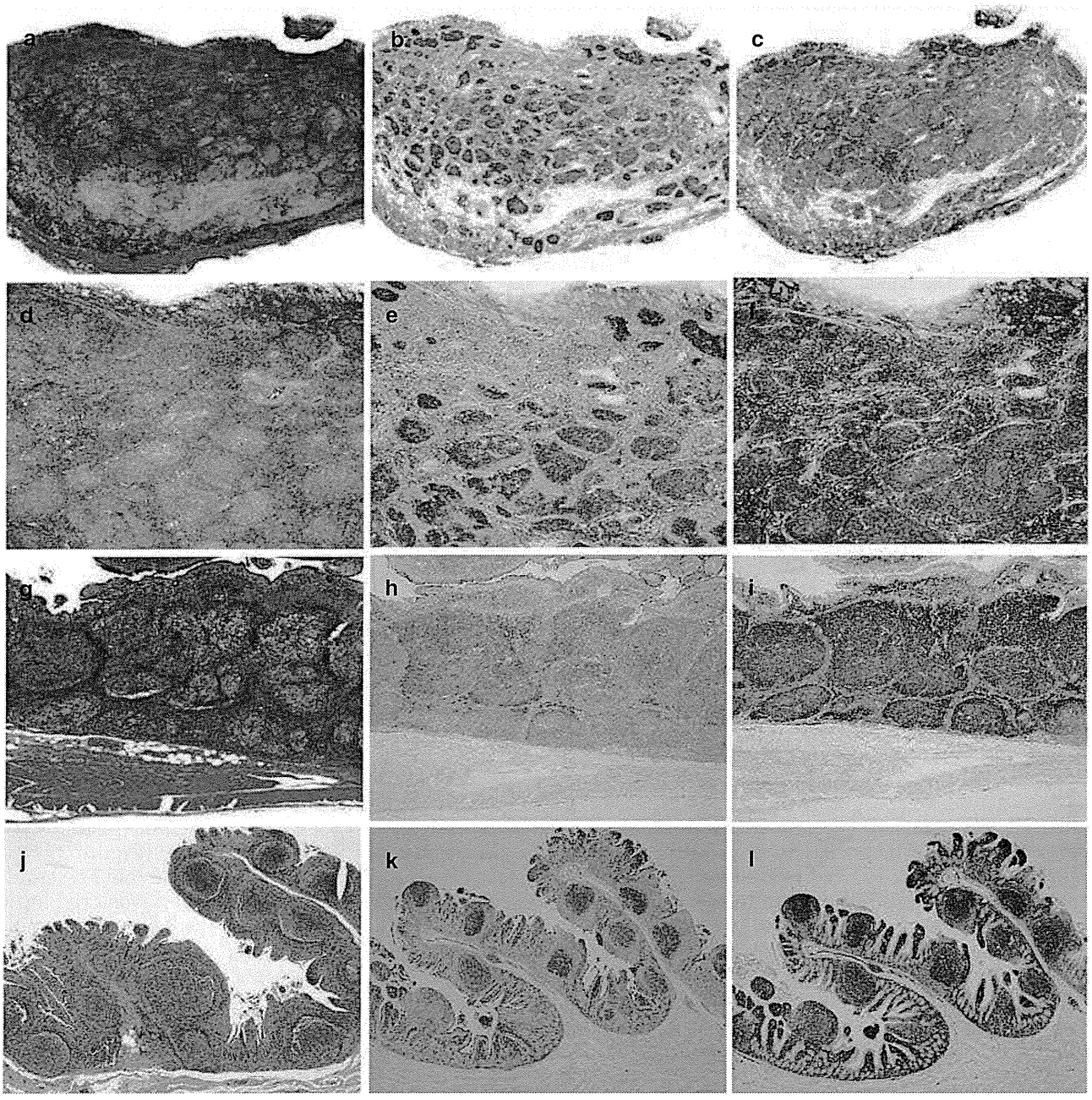

Figure 1 Pathological features of gastric, duodenal, and colonic/rectal follicular lymphoma (FL). (**a**) Gastric FL (HE stain; low power field). Tumor cells are present in the proper muscle to subserosal area. (**b**) CD10 immunostaining of gastric FL (low power field). (**c**) B-cell lymphoma 2 (BCL-2) immunostaining of gastric FL (low power field). (**d**) Gastric FL (HE. stain). Vague nodular tumor follicles are present. (**e**) CD10 immunostaining of gastric FL. Tumor cells are positive. (**f**) BCL-2 immunostaining of gastric FL. Tumor cells are positive. (**g**) Colonic FL (HE stain). Tumor cells are present in the musculature proper area. (**h**) CD10 immunostaining of colonic FL. Tumor cells are positive. (**i**) BCL-2 immunostaining of colonic FL. Tumor cells are positive. (**j**) Duodenal FL (HE stain). Tumor cells are present in the lamina propria area. (**k**) CD10 immunostaining of duodenal FL. Tumor cells are positive. (**l**) BCL-2 immunostaining of duodenal FL. Tumor cells are positive.

15 of 17 duodenal FLs as previously described (Figure 2a.[1] In contrast, among the eight stomach FLs, seven exhibited a nodal pattern and one showed an intermediate pattern (Figure 2b). Out of five patient samples in the colon and rectum, three were nodal and two were intermediate (Figures 2c and d). Statistical comparison of the expression patterns of duodenal FLs and gastric/colonic FLs showed that the distributions were significantly different ($P<0.001$).

Results of AID and BACH2 expression analyses are also shown in Table 2. Only 1 of 17 duodenal FLs expressed AID (Figure 2e), whereas 6 of 8 gastric FLs were positive for AID (Figure 2f). All colonic and rectal samples were positive for AID. BACH2 expression was comparatively different: 14 of 17

Table 2 CD21 pattern, AID, BACH2 expression and genetical study in gastrointestinal follicular lymphomas

Patient no.	*Sites*	*Stage*	*CD21 pattern*	*AID*	*BACH2*	*CD27*	*t(14;18)*	*VH usage*
1	Stomach	I	Nodal	−	+	−	+	ND
2	Stomach	IV	Intermediate	+	+	−	+	VH3-30
3	Stomach	I	Nodal	+	−	−	−	VH3-21
4	Stomach	I	Nodal	+	+	−	−	VH3-30
5	Stomach	II2	Nodal	−	+	−	+	ND
6	Stomach	I	Nodal	+	+	−	−	VH3-7
7	Stomach	I	Nodal	+	+	+	−	VH3-30
8	Stomach	II1	Nodal	+	−	−	−	VH4-34
9	Duodenum	I	Duodenal	−	−	+	ND	VH3-73
10	Duodenum	I	Duodenal	−	−	+	ND	VH3-48
11	Duodenum	IV	Duodenal	−	+	−	+	VH3-72
12	Duodenum	II2	Duodenal	−	+	+	−	VH4-34
13	Duodenum	I	Duodenal	−	(+)	+	+	VH5-a
14	Duodenum	I	Nodal	−	+	+	−	VH3-73
15	Duodenum	I	Duodenal	−	(+)	+	+	VH4-b
16	Duodenum	II2	Duodenal	−	(+)	+	+	VH4-39
17	Duodenum	II2	Duodenal	+	−	+	+	VH3-15
18	Duodenum	I	Duodenal	−	(+)	+	+	VH5-51
19	Duodenum	IV	Duodenal	−	+	−	+	VH5-51
20	Duodenum	II2	Duodenal	−	(+)	+	+	VH4-61
21	Duodenum	I	Duodenal	−	(+)	+	+	VH4-39
22	Duodenum	II2	Duodenal	−	+	+	+	VH3-73
23	Duodenum	II2	Duodenal	−	(+)	+	+	VH3-23
24	Duodenum	II2	Nodal	−	+	+	+	VH3-23
25	Duodenum	II2	Duodenal	−	+	+	+	VH3-23
26	Cecum	II2	Nodal	+	+	+	−	ND
27	Colon	I	Intermediate	+	+	−	+	ND
28	Colon	I	Nodal	+	−	−	+	VH3-33
29	Rectum	I	Intermediate	+	+	−	−	ND
30	Rectum	I	Nodal	+	−	−	+	ND

Abbreviation: AID, activation-induced cytidine deaminase; ND, not determined.
(+): positive at the periphery of tumor follicle and villi.

duodenal FL samples were positive for BACH2. Interestingly, the AID-positive sample (no. 20) was negative for BACH2. In seven samples, BACH2 was expressed at the periphery of the tumor follicle and tumor villi (Figure 2g, Table 2; shown as (+)). BACH2 was also commonly expressed in other FLs: six of eight gastric FLs were positive for BACH2 (Figure 2h) as were three of five colonic/rectal FLs.

In situ hybridization analysis of BACH2 expression confirmed the immunohistochemical findings. Tumor cells at the peripheral zone of tumor follicles and at the villi expressed BACH2 mRNA (Figures 3a and b). This pattern corresponded with the protein expression pattern. We also examined Blimp-1 expression and found no Blimp-1 expression in any of the patient samples (Table 2).

We examined differentiation in lymphoma cells using CD27 staining. As both mutated IgM^+ B-cell populations and the class-switched memory B cells share expression of the TNF-receptor superfamily member CD27, which is not expressed in unmutated naive B cells,[14,15] CD27 is thought to be a memory B-cell marker.[16] Figure 3c shows CD27 expression in the reactive lymphoid hyperplasia of the duodenum: the CD27-positive B cells or plasma cells were present at the villi and lymphoid follicle. CD27 expression is also shown in the reactive hyperplastic germinal centers of the tonsil: the positive cells were scattered in the germinal center (prominent in light zone) and interfollicular zone (Figure 3d).

As shown in Table 2, 15 of 17 duodenal FL samples strongly expressed CD27 (Figure 3e). Western blotting analysis also confirmed CD27 protein expression in duodenal FL (Supplementary Figure 1). In eight gastric and seven colonic FL samples, all samples were negative for CD27 (Figure 3f), except those of patients no. 7 and no. 26. Statistical comparison of expression patterns in duodenal FLs and nodal, gastric, and colon FLs showed that the distributions are significantly different ($P<0.001$).

IgVH Gene Usage

We could detect monoclonal bands in six of eight gastric FL samples and one of five colonic/rectal FL samples. These results are shown in Table 2. In gastric FL, five of six were VH3 and one was VH4. In duodenal FL, 9 of 17 were VH3, 5 were VH4, and 3 were VH5.

Fluorescence In Situ Hybridization

The t(14;18) translocation was detected in 13 of 15 (about 87%) duodenal FL samples, 3 of 8 (38%) gastric FLs, and 3 of 5 (60%) colon and rectal FLs (Figure 4a). In gastric FL samples, the frequency of the

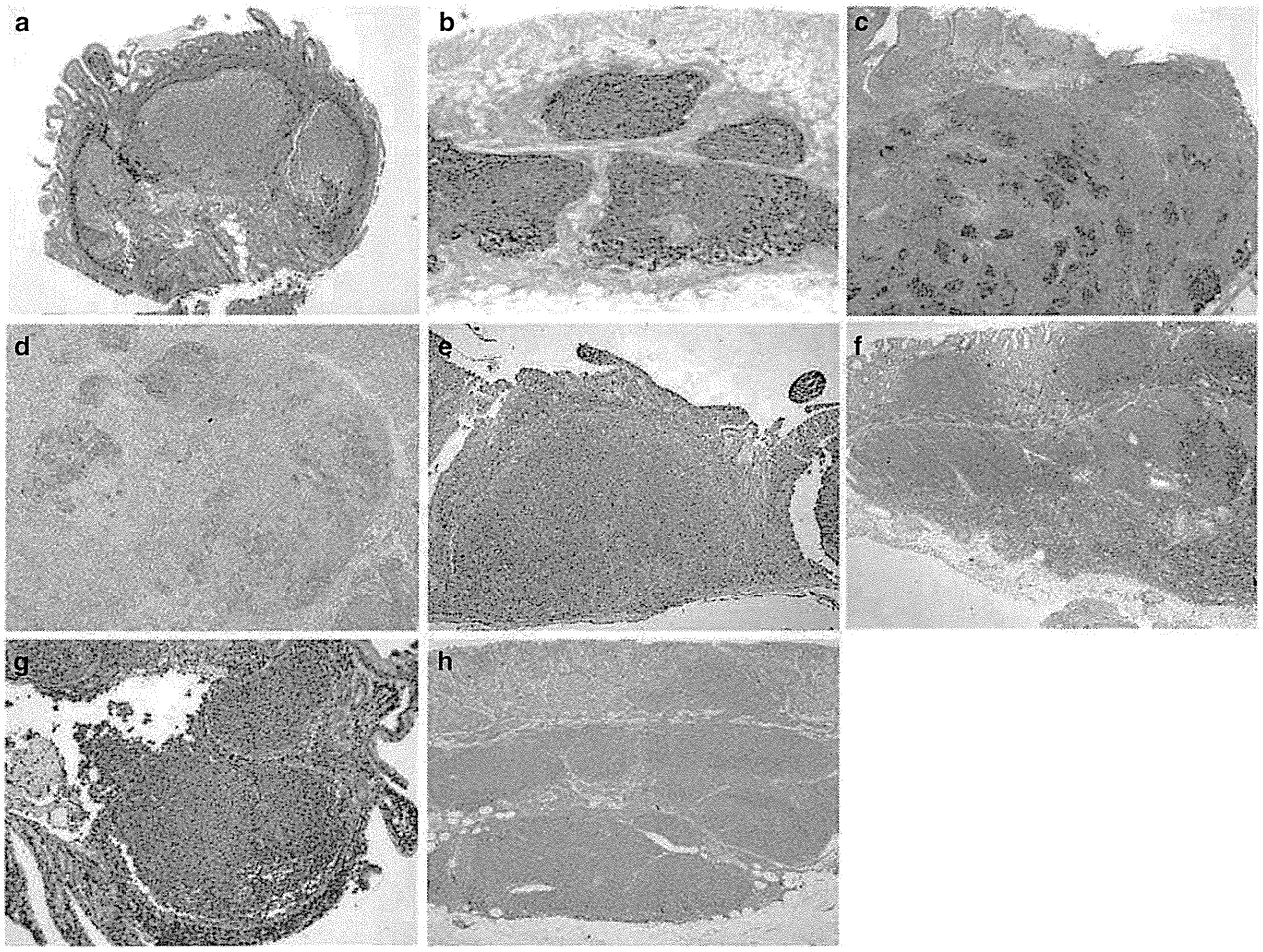

Figure 2 CD21 and AID immunohistochemistry in duodenal, gastric, and colonic FLs. (**a**) CD21 immunostaining of duodenal FL. Follicular dendritic cells (FDC) present at the periphery of tumor follicles (duodenal pattern). (**b**) CD21 immunostaining of gastric FL. FDC networks densely present in tumor follicles (nodal pattern). (**c**) CD21 immunostaining of colonic FL. FDC networks densely present in tumor follicles (nodal pattern). (**b**) Intermediate pattern of CD21 immunostaining in colonic FL. (**e**) AID immunostaining in duodenal FL. Tumor cells are negative. (**f**) AID immunostaining of gastric FL. Tumor cells are positive. (**g**) BACH2 immunostaining in duodenal FL. Periphery of tumor follicles and villi are positive, but center of tumor follicle is negative. (**h**) BACH2 immunostaining of gastric FL. Tumor follicles are positive.

translocation was significantly lower than that in duodenal FLs ($P=0.015$). Furthermore, gastric FLs with lower clinical stages (Stage I–II_1, localized tumor stage) had a lower tendency to exhibit the t(14;18) translocation (Table 2). The *IGH-BCL-2* translocation was more frequent in duodenal samples (87%) than in gastric (40%) and colonic (59%) FLs ($P=0.008$).

Discussion

Although the gastrointestinal FLs are relatively rare, accounting for 1–3.6% of all gastrointestinal lymphomas, duodenal FLs have recently been found with increasing frequency by upper gastrointestinal endoscopic examination. These FLs are characterized by lower clinical stage, lower histological grading, and better prognosis. Gine *et al*[17] reported that the frequency of clinical stage III–IV in nodal FL was 81%. Solal-Celigny *et al*[18] found a similar frequency of 78%. In our previous multicenter retrospective study, 41 of 191 patients with gastrointestinal FL (21.5%) were stage IV.[4] Histological differences between duodenal FLs and stomach and colon FLs involved tumor depth, size of individual tumor follicles and the size of the lesions. Duodenal FLs were mainly located in submucosal areas, and tumor cells were present in mucosal villi. Macroscopically, duodenal FLs typically present as small white multiple nodules. These histological differences suggest the association of a mucosal homing receptor such as $\alpha4\beta7$ as reported by Bende *et al*.[19] Most duodenal lymphoma samples are obtained by biopsy, and the assessment thus performed is considered insufficient. However, in our previous patient series, a few patients were examined by ultrasonic endoscopy. All patients who had macroscopically multiple white nodules had a limited submucosal layer. In our present series of duodenal FLs, all macroscopic types were found to be typical multiple white nodules. The patients in the present series were examined by CT and/or MRI.

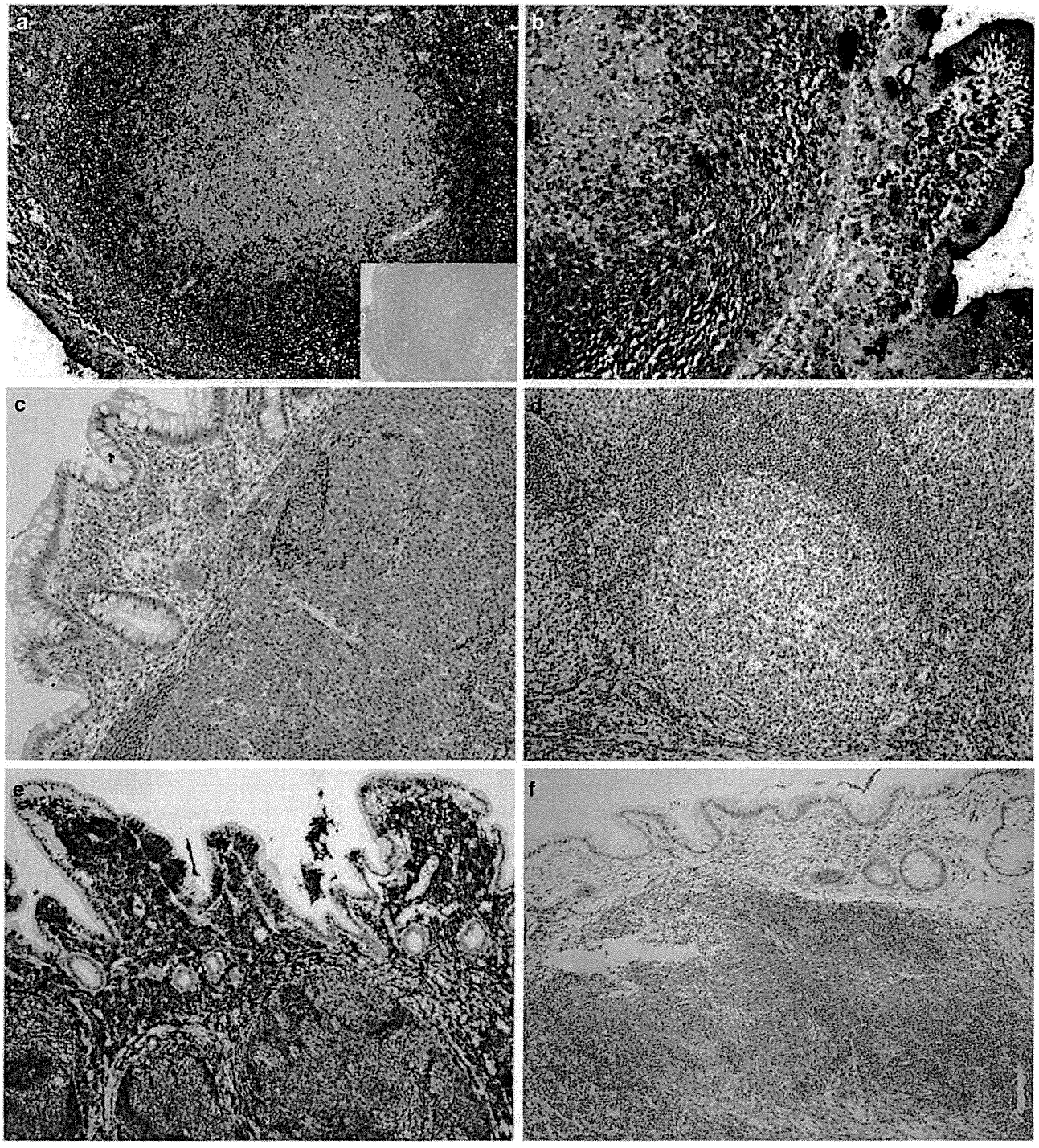

Figure 3 BACH2 and CD27 expression. (**a**) BACH2 *in situ* hybridization in duodenal follicular lymphoma (FL) sample. Levels of mRNA expression correlate with protein expression. Inset of Figure 3a shows detection of BACH2 mRNA with sense DIG-labeled probes as a negative control. (**b**) Same sample as Figure 3a. Tumor at the villi also expresses BACH2 at the mRNA level. (**c**) CD27 expression in reactive lymphoid hyperplasia of the duodenal sample. Positive cells (active B cells and plasma cells) are present at the villi. (**d**) CD27 immunostaining of reactive lymphoid hyperplasia in the tonsil sample. Positive cells are scattered in the germinal center light zone and interfollicular zone. (**e**) CD27 expression in duodenal FL. Tumor cells are strongly positive. (**f**) CD27 expression in colonic FL. Tumor follicles are negative.

We think we should examine further studies in the future.

Both normal germinal centers and nodal FLs have dense CD21-positive follicular dendritic cell networks.[20] We previously showed that duodenal FL lacked follicular dendritic cell networks, with dendritic cells distributed at the periphery of the tumor follicles.[1] In contrast, other gastrointestinal

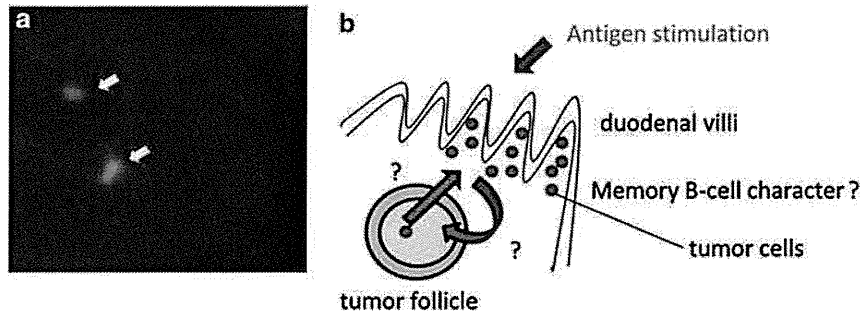

Figure 4 Fluorescence *in situ* hybridization (FISH) and schema of duodenal FL. (**a**) FISH for detection of t(14;18) in duodenal follicular lymphoma (FL) sample. IGH signal (green) and B-cell lymphoma 2 (BCL-2) signal (red) are merged (yellow: arrows). (**b**) Schema of tumor origin in duodenal FL.

tract (stomach, colon, and rectum) FLs had dense follicular dendritic cell networks similar to those of nodal FLs. The follicular dendritic cell network pattern may depend on the nature of the primary tumor. For example, we documented a patient with primary FL in the inguinal lymph node, who achieved complete remission by chemotherapy and then relapsed with lesions at duodenal and gastric sites. Interestingly, the nodal and two gastrointestinal sites showed the same follicular dendritic cell pattern (nodal pattern, data not shown). Conversely, some duodenal and nodal samples from patients presenting with systemic lymphadenopathy showed the same dendritic cell pattern (duodenal pattern, data not shown).

An important question concerns whether tumor cells invading follicles arise from the villi or whether they spread from tumor follicles to the villi. Figure 4b presents a hypothetical schema of development of duodenal FL. The VH-usage deviation and memory-cell characters strongly suggested that the presence of antigen stimulation, chemokines, and adhesion molecules probably affect tumor spreading. One hypothesis is that tumor cells originating in the villi spread to other villi and invade non-tumor follicles. Tumor cells invading non-tumor follicles disrupt the follicular dendritic cell network, as seen in follicular colonization in MALT lymphoma. Another hypothesis is that lymphoma cells from tumor follicles spread to the villi.

AID has a key role in class switching and somatic hypermutation in B cells.[5] BACH2 also has a role in these processes in B cells.[6] BACH2 and Bcl-6 suppress Blimp-1, which is a key regulator of plasma-cell differentiation.[7] We have previously reported a lack of AID expression in duodenal FLs. In the present study, 14 of 17 samples of duodenal FL expressed BACH2 protein and mRNA. In seven samples, the BACH2 pattern and the pattern of tumor cells in the villi and periphery of the tumor follicles was the same. This unique pattern was not found in nodal, gastric, or colonic FLs. This difference was quite interesting, but the mechanism by which AID and BACH2 are differentially expressed remains unclear. We cannot clearly demonstrate this association in our present study, and further studies will be required to clarify this association.

Most duodenal follicular samples expressed BACH2, and all lacked Blimp-1, which is repressed by BACH2 and Bcl-6. Thus, BACH2 might have a key role in ongoing somatic hypermutation in duodenal FLs. Sakane-Ishikawa *et al*[21] described better prognostic value of BACH2 expression in diffuse large B-cell lymphomas. Takakuwa *et al*[22] described an inhibitory effect of BACH2 on proliferation of Raji cell lines. In previous reports, BACH2 was reported to have a tumor suppressor role in B-cell lymphomas. On the other hand, AID is associated with lymphomagenesis and AID expression is related to poor prognosis in several B-cell lymphoma subtypes.[9,23,24] We do not have sufficient data for long-term follow-up of patients with duodenal FL, but based on these reports, we suggest that BACH2 expression and lack of AID expression might limit the tumor stage and lead to better prognosis in duodenal FL.

Expression of CD27 was common (15 of 17) in the duodenal FL samples. In 16 Grade 1 nodal FLs, all patient samples were negative for CD27 (data not shown). In five gastric MALT lymphoma patient samples, four samples were positive and one was negative for CD27 (data not shown). In B-cell differentiation, postgerminal center B cells, selected by affinity maturation and induced by somatic hypermutation, differentiate to plasmablasts or memory B cells.[25] CD27 is a tumor necrosis factor receptor superfamily member and a general human memory B-cell marker. In human normal intestinal mucosa, scattered secretory IgA^+ $CD27^+$ memory B cells are present in the lamina propria, but are scarce in gut-associated lymphoid tissue.[26] In duodenal FL samples, tumor cells expressed IgA, CD27, and BACH2. Thus, tumor cells differentiate to memory B cells with somatic and ongoing hypermutations. For this reason, we note that these data suggest a resemblance of duodenal FL to MALT lymphoma. $CD27^+$ memory B cells are subclassified as IgM^+IgD^+, IgM^+IgD^-, IgG^+IgA^+, and IgM-IgD^+.[27] Thus, duodenal FLs are subclassified as IgA^+ memory B-cell like. Dong HY *et al*[28] described that

CD27 did not distinguish between neoplastic B cells of naive *versus* memory type. Furthermore, Schmitter D *et al*[29] described CD27 expression in CD70-stimulated FL cells. Somatic hypermutation by itself is a feature of both follicular center and memory B cells, and CD27 is also expressed by some follicular center cells. Therefore, we should be more conservative in the precise maturational state of the duodenal FL cells. However, there might also be difference between nodal FL and duodenal FL in terms of CD27 expression.

In gastric and colonic FLs, *VH3* gene usage was frequently observed, but in our samples, we could detect too few monoclonal bands to allow comparison with duodenal samples. More samples will be required to compare VH gene usage. Translocations of t(14;18)(q32;q21) and *IGH-BCL-2* are considered to be hallmarks of FL,[29,30] but t(14;18) is present in about half the healthy samples.[31,32] In gastric FL of lower clinical stage, there were no IGH/BCL-2 translocations. These facts suggest that gastric FL may be similar to primary cutaneous follicle center lymphoma.[33,34]

In conclusion, we suggest that duodenal FL is a distinct entity among gastrointestinal FLs, by virtue of AID loss but BACH2 expression, displaying a specific CD21 pattern, and high frequency of CD27 expression.

Disclosure/conflict of interest

The authors declare no conflict of interest.

Acknowledgements

This work was supported in part by grants from the Japan Society for the Promotion Science (JSPS no. 19590348) and was supported in part by a Grant-in-Aid for Cancer Research (21-6-3) from the Ministry of Health, Labor and Welfare, Tokyo, Japan. We special thanks Ms H Nakamura, Ms M Okabe, Dr T Kunitomo, Dr A Uchiyama, Dr S Nose and Dr T Miyake for their technical assistance and preparing pathological samples.

References

1 Takata K, Sato Y, Nakamura N, *et al.* Duodenal and nodal follicular lymphomas are distinct: the former lacks activation-induced cytidine deaminase and follicular dendritic cells despite ongoing somatic hypermutations. Mod Pathol 2009;22:940–949.
2 Sato Y, Ichimura K, Tanaka T, *et al.* Duodenal follicular lymphomas share common characteristics with mucosa-associated lymphoid tissue lymphomas. J Clin Pathol 2008;61:377–381.
3 Kodama M, Kitadai Y, Shishido T, *et al.* Primary follicular lymphoma of the gastrointestinal tract: a retrospective case series. Endoscopy 2008;40:343–346.
4 Takata K, Okada H, Ohmiya N, *et al.* Primary gastrointestinal follicular lymphoma involving the duodenal second portion is a distinct entity: A multicenter, retrospective analysis in Japan. Cancer Sci 2011;102: 1532–1536.
5 Muramatsu M, Kinoshita K, Fagarasan S, *et al.* Class switch recombination and hypermutation require activation-induced cytidine deaminase (AID), a potential RNA editing enzyme. Cell 2000;102: 553–563.
6 Muto A, Tashiro S, Nakajima O, *et al.* The transcriptional programme of antibody class switching involves the repressor BACH2. Nature 2004;429:566–571.
7 Igarashi K, Ochiai K, Muto A. Architecture and dynamics of the transcription factor network that regulates B-to-plasma cell differentiation. J Biochem 2007;141:783–789.
8 Khoury JD, Jones D, Yared MA, *et al.* Bone marrow involvement in patients with nodular lymphocyte predominant Hodgkin lymphoma. Am J Surg Pathol 2004;28:489–495.
9 Leuenberger M, Frigerio S, Wild PJ, *et al.* AID protein expression in chronic lymphocytic leukemia/small lymphocytic lymphoma is associated with poor prognosis and complex genetic alterations. Mod Pathol 2010;23:177–186.
10 Takada S, Yoshino T, Taniwaki M, *et al.* Involvement of the chromosomal translocation t(11;18) in some mucosa-associated lymphoid tissue lymphomas and diffuse large B cell lymphomas of the ocular adnexa: evidence from multiplex reverse transcriptase –polymerase chain reaction and fluorescence in situ hybridization on using formalin-fixed, paraffin embedded specimens. Mod Pathol 2003;16: 445–452.
11 Mori H, Nomura T, Seno M, *et al.* Expression of phospholipid hydroperoxide glutathione peroxidase (PHGPx) mRNA in rat testes. Acta Histochem Cytochem 2001;34:25–30.
12 Nakamura N, Kuze T, Hashimoto Y, *et al.* Analysis of the immunoglobulin heavy chain gene variable region of CD5-positive and –negative diffuse large B cell lymphoma. Leukemia 2001;15:452–457.
13 Gajjar A, Hernan R, Kocak M, *et al.* Clinical, histopathologic, and molecular markers of prognosis: toward a new disease risk stratification system for medulloblastoma. J Clin Oncol 2004;22:984–993.
14 Agematsu K, Nagumo FC, Yang FC, *et al.* B cell subpopulations separated by CD27 and crucial collaboration of CD27+ B cells and helper T cells in immunoglobulin production. Eur J Immunol 1997;27: 2073–2079.
15 Klein U, Rajewsky K, Kuppers R. Human immunoglobulin IgM+IgD+ peripheral blood B cells expressing the CD27 cell surface antigen carry somatically mutated variable region genes: CD27 as a general marker for somatically mutated (memory) B cells. J Exp Med 1998;188:1679–1689.
16 Seifert M, Kuppers R. Molecular footprints of a germinal center derivation of human IgM+(IgD+) CD27+ B cells and the dynamics of memory B cell generation. J Exp Med 2009;16:2659–2669.
17 Gine E, Montoto S, Bosch F, *et al.* The follicular lymphoma international prognostic index (FLIPI) and the histological subtype are the most important factors to predict histological transformation in follicular lymphoma. Ann Oncol 2006;17:1539–1545.

18 Solal-Celigny P, Roy P, Colombat P, *et al.* Follicular lymphoma international prognostic index. Blood 2004; 1:1258–1265.
19 Bende RJ, Smit LA, Bossenbroek JG, *et al.* Primary follicular lymphoma of the small intestine: alpha4beta7 expression and immunoglobulin configuration suggest an origin from local antigen-experienced B cells. Am J Pathol 2003;162:105–113.
20 Kagami Y, Jung J, Choi YS, *et al.* Establishment of a follicular lymphoma cell line (FLK-1) dependent on follicular dendritic cell line HK. Leukemia 2001;15:148–156.
21 Sakane-Ishikawa E, Nakatsuka S, Tomita Y, *et al.* Prognostic significance of BACH2 expression in diffuse large B-cell lymphoma: A study of the Osaka lymphoma study group. J Clin Oncol 2005;23:8012–8017.
22 Takakuwa T, Luo WJ, Ham MF, *et al.* Integration of Epstein-Barr virus into chromosome 6q15 of Burkitt lymphoma cell line (Raji) induces loss of BACH2 expression. Am J Pathol 2004;164:967–974.
23 Gu X, Shivarov V, Strout MP. The role of activation-induced cytidine deaminase in lymphomagenesis. Curr Opin Hematol 2012;19:292–298.
24 Dijkman R, Tensen CP, Buettner M, *et al.* Primary cutaneous follicle center lymphoma and primary cutaneous large B-cell lymphoma, leg type, are both targeted by aberrant somatic hypermutation but demonstrate differential expression of AID. Blood 2006; 107:4926–4929.
25 Allen CDC, Okada T, Cyster JG. Germinal-center organization and cellular dynamics. Immunity 2007; 27:190–202.
26 Brandtzaeg P, Johansen FE. Mucosal B cells: phenotypic characteristics, transcriptional regulation, and homing properties. Immunol Rev 2005;206:32–63.
27 Berkowska MA, Driessen GJA, Bikos V, *et al.* Human memory B cells originate from three distinct germinal center-dependent and –independent maturation pathways. Blood 2011;118:2150–2158.
28 Dong HY, Shahasafaei A, Dorfman DM. CD148 and CD27 are expressed in B cell lymphomas derived from both memory and naïve B cells. Leuk Lymphoma 2002;43:1855–1858.
29 Schmitter D, Bolliger U, Hallek M, *et al.* Involvement of the CD27-CD70 co-stimulatory pathway in allogenic T-cell response to follicular lymphoma cells. Br J Haematol 1999;106:64–70.
30 Helen MC, David BJ, Dennis HW. Cytogenetic and molecular studies of t(14;18) and t(14;19) in nodal and extranodal B-cell lymphoma. J Pathol 1992;166: 129–137.
31 Albinger-Hegyi A, Hochreutener B, Abdou MT, *et al.* High frequency of t(14;18)-translocation breakpoints outside of major breakpoints and minor cluster regions in follicular lymphomas. Am J Pathol 2002;160: 823–832.
32 Hirt C, Dölken G, Janz S, *et al.* Distribution of t(14;18)-positive, putative lymphoma precursor cells among B-cell subsets in healthy individuals. Br J Haematol 2007;138:349–353.
33 Roulland S, Navarro JM, Grenot P, *et al.* Follicular lymphoma-like B cells in healthy individuals: a novel intermediate step in early lymphomagenesis. J Exp Med 2006;203:2425–2431.
34 Streubel B, Scheucher B, Valencak J, *et al.* Molecular cytogenetic evidence of t(14;18)(IGH;BCL2) in a substantial proportion of primary cutaneous follicle center lymphomas. Am J Surg Pathol 2006;30: 529–536.

Supplementary Information accompanies the paper on Modern Pathology website (http://www.nature.com/modpathol)

A Novel Mutation of Ribosomal Protein S10 Gene in a Japanese Patient With Diamond-Blackfan Anemia

Makoto Yazaki, MD, Michi Kamei, MD,† Yasuhiko Ito, MD,† Yuki Konno, MD,‡ RuNan Wang, MD,‡ Tsutomu Toki, MD,‡ and Etsuro Ito, MD‡*

Summary: Diamond-Blackfan anemia (DBA) is an inherited bone marrow disease. The condition is characterized by anemia that usually presents during infancy or early childhood and congenital malformation. Several reports show that DBA is associated with mutations in the ribosomal protein (RP) genes, *RPS19*, *RPS24*, *RPS17*, *RPL35A*, *RPL5*, *RPL11*, and *RPS7*. Recently, 5 and 12 patients with mutations in *RPS10* and *RPS26*, respectively, were identified in a cohort of 117 DBA probands. Therefore, we screened the DBA patients who were negative for mutations in these DBA genes for mutations in *RPS10* and *RPS26*. The present case report describes the identification of the first Japanese DBA patient with a novel mutation in *RPS10*.

Key Words: Diamond-Blackfan anemia, ribosomal protein genes, mutation in *RPS10*

(*J Pediatr Hematol Oncol* 2012;34:293–295)

Diamond-Blackfan anemia (DBA) is an inherited bone marrow disease. The condition is characterized by anemia that usually presents during infancy or early childhood, congenital malformation, and an increased incidence of cancer.[1–3] In 1999, it was reported that DBA is associated with mutations in the ribosomal protein (RP) gene, *RPS19*.[4] This mutation was identified in 25% of DBA probands and prompted the search for other RP gene mutations. Subsequently, DBA patients with mutations in *RPS24*, *RPS17*, *RPL35A*, *RPL5*, *RPL11*, and *RPS7* were reported, suggesting that DBA is a disorder of ribosomal biogenesis and/or function.[5–7] Recently, Doherty et al[8] reported 3 distinct mutations of the *RPS10* in 5 patients from a cohort of 117 DBA probands. Therefore, we screened the Japanese DBA patients who were negative for mutations in these RP genes for mutations in *RPS10* and *RPS26*. Here, we report the first Japanese DBA patient with a novel mutation in *RPS10*.

Received for publication September 14, 2011; accepted January 8, 2012.
From the *Department of Pediatrics, Nagoya City East Medical Center Moriyama Hospital; †Department of Pediatrics and Neonatology, Nagoya City University Graduate School of Medical Science, Nagoya; and ‡Department of Pediatrics, Hirosaki University Graduate School of Medicine, Hirosaki, Japan.
This study was supported in part by a grant from Health and Labor Sciences Research Grants (Research on intractable diseases) from the Ministry of Health, Labour, and Welfare of Japan.
The authors declare no conflict of interest.
Reprints: Makoto Yazaki, MD, Department of Pediatrics, Nagoya City East Medical Center Moriyama Hospital, 18-22 2-chome, Moriyama, Moriyama-ku, Nagoya 463-8567, Japan (e-mail: yazakim@mild.ocn.ne.jp).

CASE REPORT

A 6-year-old boy was referred to our hospital with anemia with no other significant cytopenia. He was an only child with no family history of anemia. He has no congenital malformations described in "classical DBA," apart from bilateral lymphangioma of the foot. His white blood cell count was 4.3×10^9/L, the erythrocyte count was 2540×10^9/L, the hematocrit was 24.6%, hemoglobin concentration was 8.3 g/dL, the mean corpuscular volume was 96.9 fl, the mean corpuscular hemoglobin was 32.7 pg, the platelet count was 278×10^9/L, and the reticulocyte count was 1.5%. The fetal hemoglobin was 1.4%. The serum iron was 93 μg/dL, the serum unsaturated iron-binding capacity was 184 μg/dL, and the serum ferritin was 9 ng/mL. The serum vitamin B12 was 850 pg/mL and the serum folic acid was 6.8 ng/mL. The serum aspartate aminotransferase was 17 U/mL, the alanine aminotransferase was 10 U/mL, and the lactate dehydrogenase was 201 U/mL. The erythropoietin level was 1170 mU/L. The serum total bilirubin was 0.5 mg/dL. The direct and indirect Coombs' tests were negative. The anti-B19 parvovirus immunoglobulin M and immunoglobulin G antibodies were negative. Bone marrow aspiration showed that the cellularity was slightly hypoplastic (78500/μL), with a paucity of erythroid cells (16.8%; macrocytic-basophilic erythroblasts, 0.4%, noromocytic-basophilic erythrobalasts, 1.2%, noromocytic-polychromic erythroblasts, 10.4%, normocytic-orthochromic erythroblasts, 4.8%), but the morphology was normal. It showed that myeloid cells (34.4%) have no abnormalities associated with myelodysplastic syndromes. Lymphoid cells (38%) and megakaryocytes were normal. Cytogenetic analysis showed no chromosomal abnormality. On the basis of these findings, DBA was diagnosed in this patient.[1] The patient responded to oral steroids but not to cyclosporine. A small dose of prednisolone (0.18 to 0.23 mg/kg/d) were given to maintain an erythrocyte count of 2500×10^9/L, a hemoglobin concentration of 8.0 g/dL, and his daily activities. The most distressing complication has been obesity. He has never received blood transfusion.

At 22 years of age, analysis of RP genes was performed. Informed consent was obtained according to the guidelines set out by Hirosaki University Graduate School of Medicine. Initially, the patient was screened for mutations in the 8 genes known to be associated with DBA, *RPS19*, *RPS24*, *RPS17*, *RPL5*, *RPL11*, *RPL35A*, *RPS10*, and *RPS26*, using high-resolution amplicon melting analysis. He was also screened for *RPS14* mutations, which are a causative gene for 5q-syndrome. The results showed a separated signal derived from the heteroduplex polymerase chain reaction product from the third exon of *RPS10*. Direct sequencing analysis of the polymerase chain reaction product and the cloned amplicon identified a heterozygous mutation (283_306delinsTGCC) (Fig. 1). This mutation resulted in a frameshift at codon 95 and a "stop" at codon 100 (Fig. 2).

DISCUSSION

Nine RP genes, *RPS19*, *RPS24*, *RPS17*, *RPL5*, *RPL11*, *RPL35A*, *RPS14*, *RPS10*, and *RPS26*, were screened in 64 Japanese probands with DBA. Screening identified 8, 6, and 3 patients with mutations in *RPS19*, *RPL5*, and *RPL11*, respectively, and a single patient each with a mutation in *RPS17*, *RPS10*, and *RPS26*[9] and

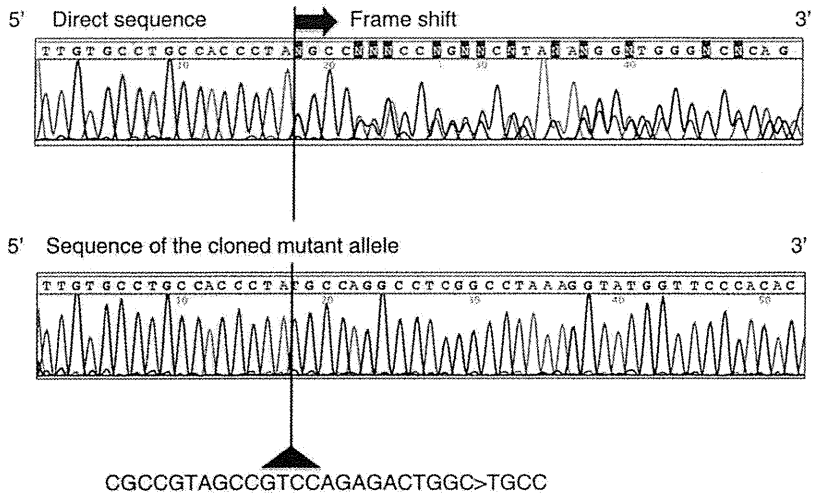

FIGURE 1. Sequence changes and frameshift in the *RPS10*. Direct sequencing showed a separated signal derived from the heteroduplex polymerase chain reaction product from the third exon of *RPS10*. Sequencing of the cloned mutant allele identified a heterozygous mutation (c.283_306delinsTGCC) and frameshift.

(unpublished data). In total, 20 (31.3%) of the Japanese DBA patients had mutations in RP genes. This is a slightly lower frequency than that reported in Western countries, although the data from both populations are based on relatively low numbers of patients, and data showing significant differences between populations are lacking.

The RPSP10 gene is located on chromosome 6 and contains 6 exons, with the start codon in exon 2. *RPS10* encodes a protein of 165 amino acids, which is a component of the 40S ribosomal subunit. To our knowledge, this is the first report of a Japanese DBA patient with a mutation in *RPS10*. The mutation (283_306delinsTGCC) results in a frameshift at codon 95 and the premature termination of codon 100. This novel mutation has not been reported in the literature. Doherty et al[8] identified 3 heterozygous sequence changes in *RPS10* in 5/117 probands, with no evidence of mutations in any of the known DBA genes. One sequence change was a missense mutation 3G > A (Met1 to Ile), which eliminates the start codon. The next downstream start codon is located at nucleotide position 61 to 63 and is predicted to start translation of a truncated protein. Another mutation was c.260_261insC, which results in a frameshift at codon 87 and a "stop" at codon 97. Three other probands contained a common nonsense mutation, c.337C > T, causing an Arg113 "stop." In our case, the mutation seems to be the result of both a deletion and an insertion. These mutations are very rare in DBA. To understand the mechanism of mutagenesis, we examined *RPS10* psuedogenes (*PRS10P1* to *RPS10P31*) to see if this mutation arose from interlocus gene conversion. However, we could find no evidence that the mutation arose due to gene conversion. The authors estimated that *RPS10* mutations were present in about 2.6% of the DBA population. Although more information is needed to estimate the incidence of *RPS10* mutations in Japanese DBA patients, the frequency of *RPS10* mutations in the Japanese population was similar to that in Western countries. All the *RPS10* mutations observed in patients with DBA, including our case, are nonsense or frameshift mutations. Nonsense and frameshift mutations are likely to be pathogenic in the majority of cases; however, determining the pathogenicity of a particular missense mutation may be difficult.

The RPS19 protein plays an important role in 18S rRNA maturation in both yeast and human cells.[10–13] Other

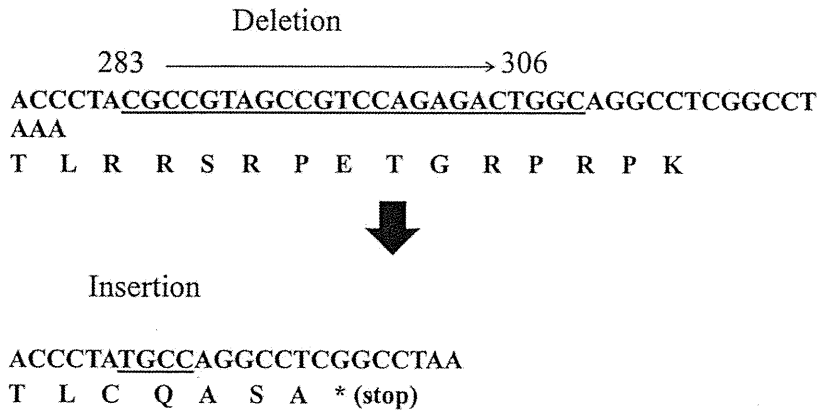

FIGURE 2. Deletion and insertion of this patient in *RSP10*. The c.283_306delinsTGCC mutation resulted in a frameshift at codon 95 and a "stop" at codon 100.

studies demonstrate alterations of pre-RNA processing and small or large ribosomal subunit synthesis in human cells with *RPS24*, *RPS7*, *RPL35A*, *RPL5*, and *RPL11* deficiency.[14–16] Increased apoptosis has been demonstrated in hematopoietic cell lines and bone marrow cells deficient in RPS19 and RPL35A.[14,17,18] Imbalances in p53 family proteins have been suggested as a mechanism of abnormal embryogenesis and anemia in zebrafish upon perturbation of RPS19 expression.[19] Also, the DBA phenotype in mice was ameliorated by knockdown of p53.[20] We hope to use hematopoietic progenitor cells to investigate why mutations in *RPS10* affect erythropoiesis in DBA patients.

Patients with "classical DBA" fulfill all the major diagnostic criteria, including anemia presenting before the first birthday.[1] However, a definitive diagnosis of DBA is often difficult because of incomplete phenotypes and a wide variation in clinical expression. This particular patient presented with macrocytic anemia at 6 years of age, with no family history and none of the congenital anomalies described for "classical DBA." The identification of pathogenic mutations in *RPS10* provides a definitive diagnosis of DBA in this patient. Although the use of molecular diagnostic techniques is essential to establish a definitive diagnosis and research the cause of DBA, such a diagnosis in only obtained for 30% to 40% of patients. Therefore, it is important to identify all genes that cause DBA if we are to improve the efficiency of molecular diagnostic techniques and understand the pathogenesis of DBA.

REFERENCES

1. Vlachos A, Ball S, Dahl N, et al. Diagnosing and treating Diamond Blackfan anaemia: results of an international clinical consensus conference. *Br J Haematol.* 2008;142:859–876.
2. Gazda HT, Sieff CA. Recent insights into the pathogenesis of Diamond-Blackfan anemia. *Br J Haematol.* 2006;135:149–157.
3. Flygare J, Karlsson S. Diamond-Blackfan anemia: erythropoiesis lost in translation. *Blood.* 2007;109:3152–3160.
4. Draptchinskaia N, Gustavsson P, Andersson B, et al. The gene encoding ribosomal protein S19 is mutated in Diamond-Blackfan anemia. *Nat Genet.* 1999;21:169–175.
5. Gazda HT, Grabowska A, Merida-Long LB, et al. Ribosomal protein S24 gene is mutated in Diamond-Blackfan anemia. *Am J Hum Genet.* 2006;79:1110–1118.
6. Cmejla R, Cmejlova J, Handrkowa H, et al. Ribosomal protein S17 gene (RPS17) is mutated in Diamond-Blackfan anemia. *Hum Mutat.* 2007;28:1178–1182.
7. Ito E, Konno Y, Toki T, Terui K. Molecular pathogenesis in Diamond-Blackfan anemia. *Int J Hematol.* 2010;92:413–418.
8. Doherty L, Sheen MR, Vlachos A, et al. Ribosomal protein genes RPS10 and RPS26 are commonly mutated in Diamond-Blackfan anemia. *Am J Hum Genet.* 2010;86:222–228.
9. Konno Y, Toki T, Tandai S, et al. Mutations in the ribosomal protein genes in Japanese patients with Diamond-Blackfan anemia. *Haematologica.* 2010;95:1293–1299.
10. Lēger-Silvestre I, Caffrey JM, Dawaliby R, et al. Specific role for yeast homologs of the Diamond Blackfan anemia-associated RPS19 protein in ribosome synthesis. *J Biol Chem.* 2005;280:38177–38185.
11. Choesmel V, Bacquevulle D, Rouquette J, et al. Impaired ribosome biogenesis in Diamond-Blackfan anemia. *Blood.* 2007;109:1275–1283.
12. Flygare J, Aspesi A, Bailey JC, et al. Human RPS19, the gene mutation in Diamond-Blackfan anemia, encodes a ribosomal protein required for the maturation of 40S ribosomal subunits. *Blood.* 2007;109:980–986.
13. Idol RA, Robledo S, Du HY, et al. Cells depleted for RPS19, protein associated in Diamond-Blackfan anemia, show defects in 18S ribosomal RNA synthesis and small ribosomal subunit production. *Blood Cell Mol Dis.* 2007;39:35–43.
14. Farrar JE, Nater M, Caywood E, et al. Abnormalities of the large ribosomal subunit protein, Rpl35a, in Diamond-Blackfan anemia. *Blood.* 2008;112:1582–1592.
15. Gazda HT, Sheen MR, Vlachos A, et al. Ribosomal Protein L5 and L11 mutations are associated with cleft palate and abnormal thumbs in Diamond-Blackfan anemia patients. *Am J Hum Genet.* 2008;83:769–780.
16. Choesmel V, Fribourg S, Aguissa-Tourē AH, et al. Mutation of ribosomal protein RPS24 in Diamond-Blackfan anemia results in ribosome biogenesis disorder. *Hum Mol Genet.* 2008;17:1253–1263.
17. Perdahl EB, Naprstek BI, Wallace WC, et al. Erythroid failure in Diamond-Blackfan anemia is characterized by apoptosis. *Blood.* 1994;83:645–650.
18. Miyake K, Utsugisawa T, Flygare J, et al. Ribosomal protein S19 deficiency leads to reduced proliferation and increased apoptosis but does not affect terminal erythroid differentiation in a cell line model of Diamond-Blackfan anemia patients. *Stem Cells.* 2008;26:323–329.
19. Danilova N, Sakamoto KM, Lin S. Ribosomal protein S19 deficiency in zebrafish leads to developmental abnormalities and defective erythropoiesis through activation of p53 protein family. *Blood.* 2008;112:5228–5237.
20. McGowan KA, Li JZ, Park CY, et al. Ribosomal mutations cause p53-mediated dark shin and pleiotropic effect. *Nat Genet.* 2008;40:963–970.

5．骨髄不全症候群におけるテロメア制御異常

山口　博樹[1]・檀　和夫[2]
Yamaguchi Hiroki　Dan Kazuo

日本医科大学 血液内科 [1]講師 [2]主任教授

Summary　Dyskeratosis congenita（DKC）は，網状色素沈着，爪の萎縮，舌などの粘膜白斑症を伴う遺伝性骨髄不全症である。テロメラーゼ複合体を構成する遺伝子群，Shelterin 複合体を構成する *TINF2*，テロメラーゼ複合体を核内の Cajalbody に移行させる *TCAB1* が DKC の責任遺伝子として同定された。DKC は，これらの遺伝子変異が原因のテロメア制御不全に，世代促進や加齢が加わることでテロメアが短縮化し，その結果造血幹細胞などの増殖能に障害が生じて発症すると考えられている。しかし，依然として確立した治療法はなく，さらなる病態の解析による新たな治療法が期待される。

はじめに

テロメアは染色体の末端部位に存在する繰り返し配列を持つ DNA（ヒトでは 5'-TTAGGG-3'）と，そこに局在するテロメラーゼ複合体や Shelterin 複合体などの種々の蛋白質から構成されている[1]。テロメアはその構造から，他の要因で受けた DNA 切断末端と区別され，DNA の分解や修復から染色体を保護し，物理的および遺伝的な安定性を保つ働きをしている[1]。

ヒトなどの動物組織から取り出した培養細胞は，複数回の分裂を繰り返すとテロメア長が短縮化し細胞分裂が停止する，細胞老化という現象が認められる[2, 3]。これは細胞分裂の際に DNA 複製が行われるが，リーディング鎖は完全にコピーされるのに対して，ラギング鎖は最終の岡崎フラグメントから約 200 bp 離れたところに複製のためのプライマーが合成されるため，3' 末端の一部はコピーが不完全となるためである[1, 4, 5]。また，仮に偶然 3' 末端にプライマーが合成されても，複製後プライマーは DNA に変換されないため，テロメアの短縮化は避けられない[1, 4, 5]。しかし，造血幹細胞や生殖細胞などでは，テロメラーゼによるテロメア長の伸長補正が行われるため，常に細胞分裂が可能である[1]。

近年，このテロメア長の伸長補正の障害が，Dyskeratosis congenita（DKC），一部の再生不良性貧血や骨髄異形性症候群，特発性肺線維症の

DKC (Dyskeratosis congenita)

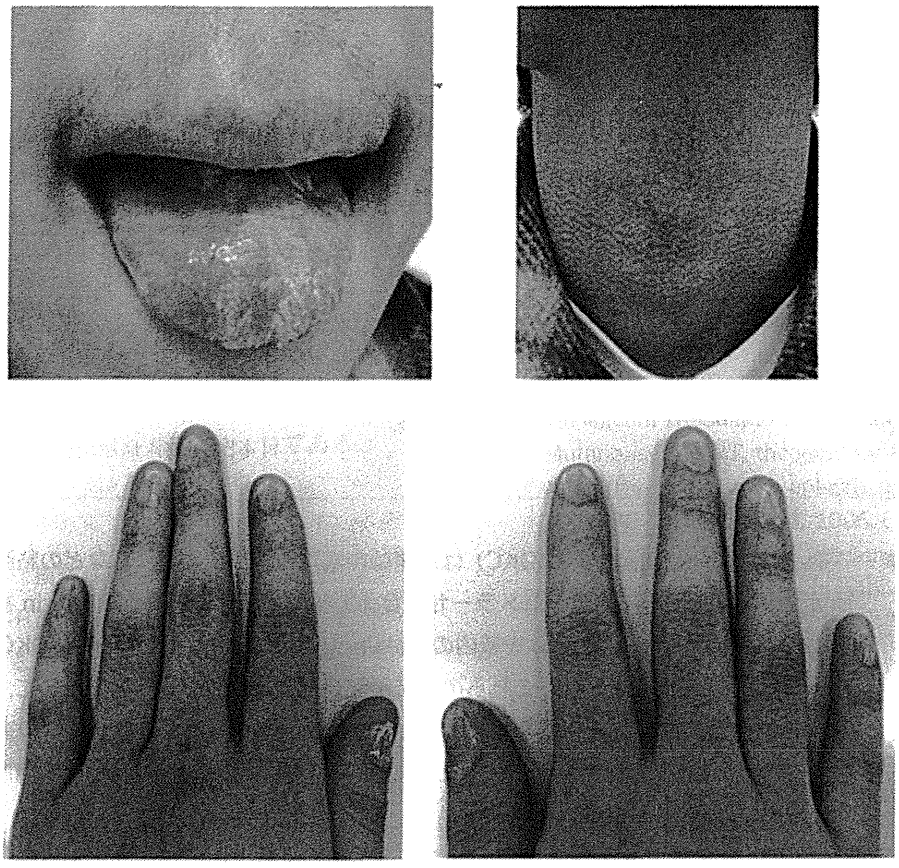

図1　DKCの特徴的身体所見

DKCの特徴的身体所見を示す。左上段：舌の粘膜白斑症，右上段：網状色素沈着，下段：爪の萎縮。（筆者提供）

原因と同定され，さらには猫鳴き症候群，急性骨髄性白血病，肝硬変などの病態への関与も示唆されている[6~9]。本稿では，DKCなどの骨髄不全症候群とテロメア制御異常に関して概説する。

1．DKCにおけるテロメア関連遺伝子異常

DKCは網状色素沈着，爪の萎縮，舌などの粘膜白斑症を伴う骨髄不全症（Bone marrow failure：BMF）で，10歳前後までに約80%以上の症例にこれらの特徴的身体所見が付随しBMFを発症する（**図1**）[7]。そして上記以外にも，精神発育遅滞，肺疾患，低身長，歯の異常，食道狭窄，頭髪の喪失，白髪などの多彩な合併症が15～25%の症例に認められ，また8%の症例に皮膚，上咽頭，消化管の扁平上皮癌や腺癌などの悪性腫瘍や，骨髄異形成症候群（MDS），Hodgkin病，急性骨髄性白血病などの造血器腫瘍の発生が認められる[7]。

遺伝型式はX連鎖劣性遺伝が約35%，常染色体優性遺伝が約15%，常染色体劣性遺伝が数%

BMF（Bone marrow failure；骨髄不全症）　MDS（骨髄異形成症候群）

表1　テロメア関連遺伝子変異と疾患

遺伝子（蛋白）	染色体存在部位	DKCにおける変異頻度	変異のtype	疾患
Telomerase				
TERC	3q21-28	5～10%	Heterozygous	AD-DKC, AA, ET, MDS PNH, PF
TERT (TERT)	5p15.33	5%	Heterozygous	AD-DKC, AA, HHS, PF
			Biallelic	AR-DKC, HHS
DKC1 (Dyskerin)	Xq28	30%	Heterozygous	X-linked DKC, HHS
NHP2 (NHP2)	5q35.3	< 1%	Biallelic	AR-DKC
NOP10 (NOP10)	15q14-q15	< 1%	Heterozygous	AR-DKC
TCAB1	17p13.1	< 1%	Biallelic	AR-DKC
Shelterin				
TINF2 (TINF2)	14q11.2	10～15%	Heterozygous	AD-DKC, AA, HHS, RS

AD-DKC：常染色体優性遺伝型DKC，AA：再生不良性貧血，ET：本態性血小板血症，MDS：骨髄異形成症候群，PNH：発作性夜間ヘモグロビン尿症，PF：肺線維症，HHS：Hoyeraal-Hreidarsson syndrome，X-kinked DKC：X連鎖劣性遺伝型DKC，AR-DKC：常染色体劣性遺伝型DKC，RS：Revesz Syndrome

DKCは表に記載した遺伝子変異によりテロメアが短縮化し，その結果造血幹細胞などの増殖能に障害が生じ，骨髄不全症や網状色素沈着，爪の萎縮，舌などの粘膜白斑症の症候が形成されると考えられている。（文献7より改変）

に認められるが，残りの約40%近くが型式不明である[7]。近年，テロメラーゼ複合体を構成する遺伝子群である，*DKC1*，*telomerase RNA component*（***TERC***），*telomerase reverse transcriptase*（***TERT***），*NOP10*，*NHP2*，Shelterin複合体を構成する*TRF-interacting nuclear protein*（***TINF2***），テロメラーゼ複合体を核内のCajalbodyに移行させる*TCAB1*がDKCの責任遺伝子として同定された（**表1**）[6～10]。DKCはこれらの遺伝子の変異によりテロメアが短縮化し，その結果造血幹細胞などの増殖能に障害が生じ，前述の症候が形成されると考えられている[7]。

また，DKCの発症年齢，随伴症状，造血障害の有無とテロメアの短縮化の程度には相関がみられ，後述のDKCの重症型と考えられているHoyeraal-Hreidarsson syndrome（**HHS**）は，DKCと比較してテロメアの短縮が著しいと報告されている[11]。

HHSは男児の幼時期に骨髄不全症を発症する遺伝性疾患である。骨髄不全症以外には小頭症，小脳低形成，成長発達遅延，顔貌異常，B細胞とNK細胞数の低下，細胞性免疫不全を合併し，大多数の症例は10歳前後で死亡する[12]。遺伝型式の大多数はX連鎖劣性遺伝の男児とされてきたが，女児のHHSも報告されるようになった[12]。最近の報告ではHHSの1/3の症例は女児で，その遺伝型式は常染色体劣性遺伝とされている[11]。HHSは独立した疾患として考えられていたが，その後HHSに*DKC1*，*TERT*などのテロメア制御遺伝子変異が発見され，DKCの重症型と考えられるようになった[12, 13]。

2．X連鎖劣性遺伝型のDKC

*DKC1*遺伝子（***DKC1***）は，染色体Xq28上にコードされ，X連鎖劣性遺伝型のDKCの原因遺伝子である。*DKC1*によって翻訳されるDyskerinは核内蛋白のsmall nucleolar RNAs（**snoRNA**）

TERC（*telomerase RNA component*）　***TERT***（*telomerase reverse transcriptase*）　***TINF2***（*TRF-interacting nuclear protein*）
HHS（Hoyeraal-Hreidarsson syndrome）　***DKC1***（*DKC1*遺伝子）　**snoRNA**（small nucleolar RNAs）

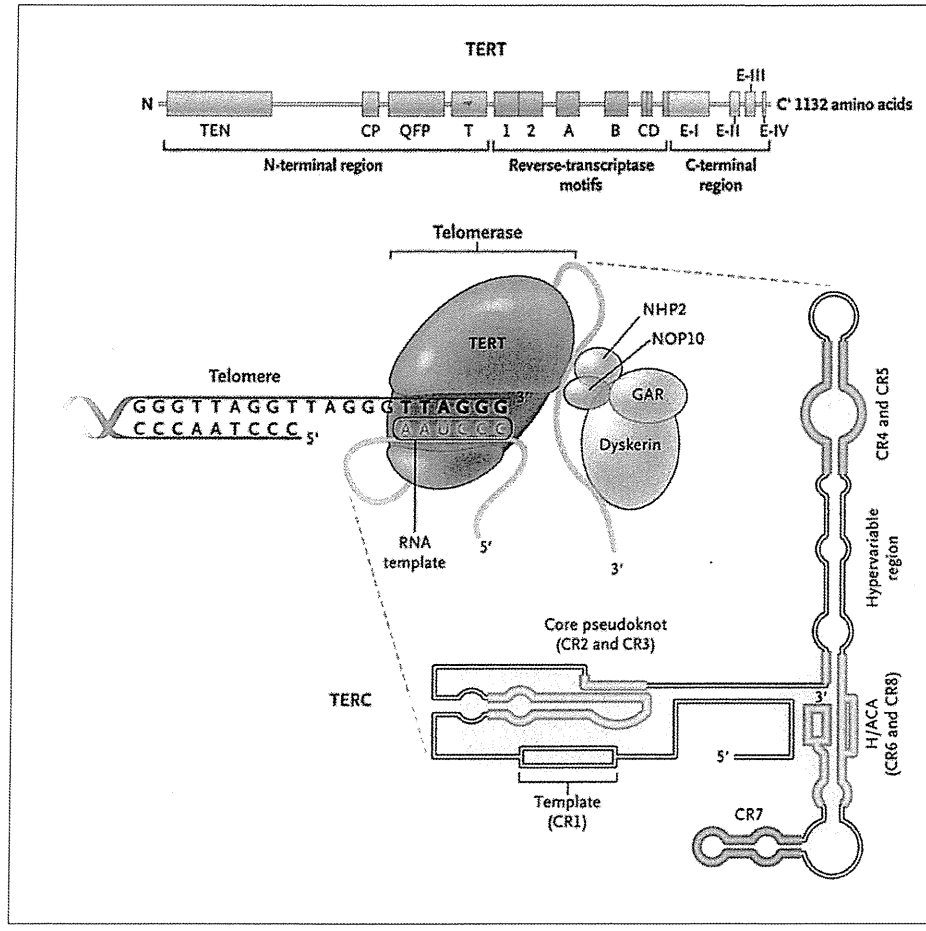

図2　テロメラーゼ複合体

TERC は自身で2次構造を形成し，5'側の pseudoknot ドメインと CR4-CR5 ドメインは TERT と結合し，テロメラーゼ活性に関与している。一方，3'側の boxH/ACA ドメインは Dyskerin などの snoRNA 蛋白と結合し，CR7 ドメインは small Cajalbody RNAs 蛋白 (scaRNAs) と CAB box を介して結合することで，テロメラーゼ複合体の processing や stability に関与している。　(文献9より改変)

の一つで，boxH/ACA ドメインを持ち，他の snoRNA である NOP10，NHP2，GAR1 と複合体を形成し，ribosomal RNA (**rRNA**) の processing や pre rRNA の転写産物の翻訳後修飾 (pseudouridylation) に関与していると考えられている[14]。また，Dyskerin を含む snoRNA 複合体は *TERC* の boxH/ACA ドメインと結合し，テロメラーゼ複合体の processing と安定化の役割を果たしている (**図2**)[14]。

X連鎖型の DKC はこの *DKC1* の変異によって引き起こされると考えられているが，その変異の大多数は point mutation で，large deletion やスプライス変異は稀である。これは *DKC1* の knockout マウスは胎性致死を起こすことから，Dyskerin は細胞の生存に必須の蛋白であるためではないかと予想される[15]。*DKC1* の変異は

rRNA (ribosomal RNA)

exon 3，4，10，11，12に集中しており，中でもexon 11のPUA pseudouridin合成酵素モチーフ上には多くの変異が認められる。特に，*DKC1*変異の約30%に認められるA353Vはhotspotとかんがえられており，*TERC*とsnoRNAのaccumulation，テロメラーゼ活性，rRNA processingやpseudouridylationに障害を与え，DKCの病態への関与が示されている[16]。また，TruB pseudouridin合成酵素モチーフの存在する領域の変異であるS121GやR158Wが，DKCの重症型と考えられているHHSの表現型を示すことは興味深い点である[12]。しかし，DKCとHH両者に認められる変異も存在し，変異部位とDKCの重症度，HHSとの関連には不明な点が多い[11,12]。さらに，*DKC1*のpromoter領域には3つのGC-rich *cis*-elementsが存在し，Sp1とSp3により*DKC1*の発現が調節されている。そのSp1 binding siteの変異である－141C/GがDKC1の発現量を低下させDKCを発症させることが報告されており，DKCはDyskerinの変異による質的な異常だけでなく，量的な異常でも発症することが示唆されている[17]。

DKCのモデルとしては，*DKC1*のexon 12-15の欠損またはexon 15のみ欠損するDyskerin hypomorphic変異マウスでの解析が行われている[18]。この*DKC1*の発現を著しく低下させたモデルマウスでは，最初の第2世代目までにDKCの表現型が再現される。興味深いことに，DKCの表現型が再現される第2世代目では，rRNAのprocessingや*mTERC*の発現とテロメラーゼ活性の低下は認められるが，テロメア長の短縮は認められず，第4世代目になってようやくテロメア長の短縮化が認められる[18]。このことは，DKCの病態の形成にリボゾームの機能障害が関与していることを示している。

3．常染色体優性遺伝型のDKC

1）*TERC*と*TERT*遺伝子変異

常染色体優性遺伝型のDKCの原因遺伝子としては，テロメラーゼ複合体の*TERC*と*TERT*が同定されている。*TERC*は染色体3q21-28上にコードされ，蛋白に翻訳されない451 bpのRNAとしてテロメア伸展における鋳型の役割をしている[1,19]。*TERC*は自身で2次構造を形成し，5'側のpseudoknotドメインとCR4-CR5ドメインは，TERTと結合してテロメラーゼ活性に関与している[1,19]。一方，3'側のboxH/ACAドメインはDyskerinなどのsnoRNA蛋白と結合し，CR7ドメインはsmall Cajalbody RNAs蛋白（scaRNAs）とCAB boxを介して結合することで，テロメラーゼ複合体のprocessingやstabilityに関与している（**図2**）[1,19]。scaRNAs蛋白は核内のCajalbodyに存在し，snoRNAと同様にrRNAに対してのpseudouridylationやmethylationなどを修飾する機能があると考えられている[20]。一方，テロメラーゼ複合体において逆転写酵素の役割をもつ*TERT*は，染色体5p15にコードされ*TERC* bindingの機能があるN-terminus，7つのconserved motifsがあり逆転写活性をもつreverse transcriptase（RT）と，telomerase multimerizationの機能があるC-terminuの3つのregionで構成されている（**図2**）[1,19]。

常染色体優性遺伝型のDKCの特徴は，X連鎖劣性遺伝型のDKCと比較して症状や検査所見の異常が軽度である症例が多いということである[6~8]。これは，後述の不全型DKCでは*DKC1*変異は認められず，その大多数において*TERC*や*TERT*の変異が認められることからも推測される[6~9]。*In vitro*の機能解析では，*TERC*の鋳型となる配列の変異はdominant negative効果でテロ

scaRNAs (small Cajalbody RNAs蛋白)　RT (reverse transcriptase)

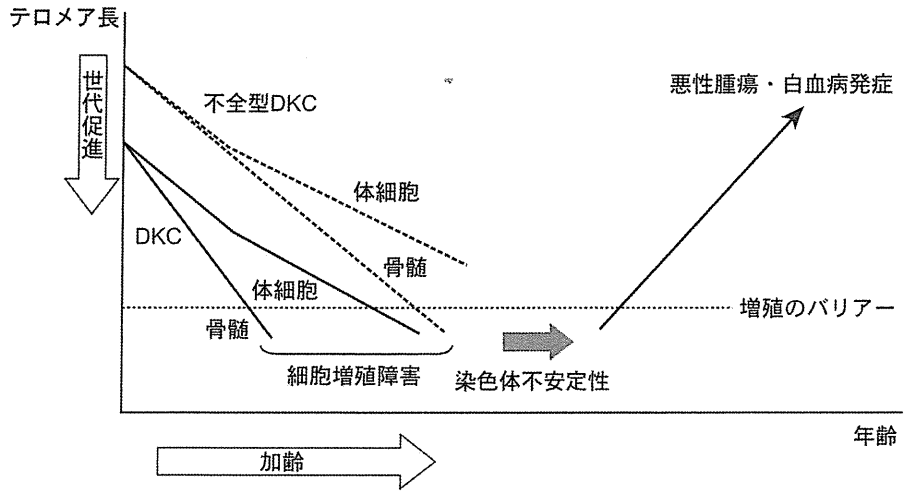

図3　DKCの発症機序

DKCはテロメア関連遺伝子変異によるテロメア伸長補正の障害，世代促進，加齢が病態の形成に重要である。テロメア関連遺伝子変異のテロメア補正の障害が軽度の場合や，世代促進や加齢が進んでいない場合は，DKCの特徴的身体所見が出現しないで不全型DKCを発症する可能性がある。（筆者作成）

メラーゼ活性を減弱させるが，その他の変異はhaploinsufficiency効果を示し，テロメラーゼ活性の減弱の程度は弱く，このことが常染色体優性遺伝型のDKCの症状や検査所見の異常が軽度である一つの理由として考えられている[21~23]。また，モデルマウスでも同様の結果が得られており，前述の*DKC1*低発現マウスが第2世代目までにDKCの表現型が再現されるのに対して，*TERC*や*TERT*のknockoutマウスでは1世代ごとにテロメアの短縮が認められ，世代が進むにつれて前者では精子形成の欠損，造血細胞の増殖障害などを，後者では消化管粘膜上皮のアポトーシスなどが認められるようになるが，DKCの表現型は示さない[6, 8, 24]。

しかし一方で，*TERT*の変異を有するHHSの表現型を示す症例が存在しており，これらの遺伝子変異の部位や両アレルの変異の存在などがDKCの表現型に関与している可能性がある[25]。また，*TERC*の変異が認められるDKCの家系においては，世代が進むにつれて発症年齢が早まり，テロメア長の短縮も顕著になってくる世代促進現象が認められる[26]。このことは前述のマウスモデルでも同様の結果が得られており，DKCの表現型には世代の促進が重要な役割をしていると予想される[18, 24]。そして，Fanconi貧血などの他の遺伝性骨髄不全症の発症年齢中央値が10歳以下なのに対して，DKCは15歳前後で，半数近くの症例が成人で診断されていることから，世代促進だけでなく加齢もDKCの表現型に重要な役割をしていると予想される（**図3**）[27]。

2）*TINF2*遺伝子変異

近年，染色体14q11.2上に存在する*TINF2*の変異が常染色体優性遺伝型のDKCで同定された[28, 29]。*TINF2*はShelterin複合体を構成するTIN2をコードしている[30]。テロメアDNAの最末端部位は，DNAの3'末端が突出（オーバーハング）して一本鎖になっている。また，哺乳類のテロメアは折り曲がってTループと呼ばれる構造を

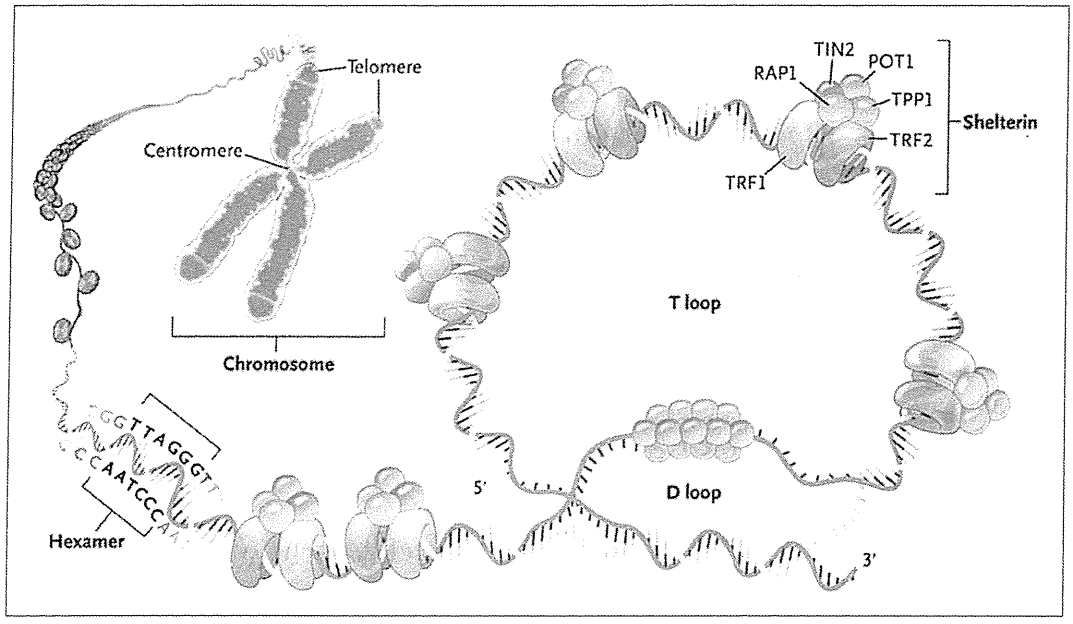

図4　Shelterin 複合体

テロメア DNA の最末端部位は，DNA の 3' 末端が突出（オーバーハング）して一本鎖になっている。また，哺乳類のテロメアは折り曲がってTループと呼ばれる構造をとり，このオーバーハングした一本鎖 DNA は，その上流のテロメア二本鎖の中に入り込みDループを構成する。Shelterin 複合体は，この特異的な構造形成や保護などを行っている。（文献９より改変）

とり，このオーバーハングした一本鎖 DNA はその上流のテロメア二本鎖の中に入り込み，Dループを構成する[30]。Shelterin 複合体はこの特異的な構造形成や保護などを行っているが，Shelterin 複合体は二本鎖 DNA と結合する TRF1 と TRF2，一本鎖 DNA に結合する POT1，これらの蛋白を結合させ複合体を形成する役割をもつ TIN2，RAP1，TPP1 で構成されている（図4）[30]。

TINF2 の変異は DKC の約 10 ～ 15%に認められ，DKC1 の次に多く認められる遺伝子変異である[7]。*TINF2* の変異の多くはヘテロの point mutation で，半数以上が TRF1 との結合ドメインの中のコドン 282arginine の変異である。また，その他の変異の大多数もコドン 282 近傍の変異であり，この領域が *TINF2* の機能として重要であることを示唆している。*TINF2* の変異の機能に関しては不明な点が多くあるが，*TINF2* の knock out マウスは胎性致死となることから，*TINF2* は細胞の生存に必須の蛋白であることが予想される[31]。また，*TINF2* の conservation region の変異は，TRF1 との結合ができなくなることで Shelterin 複合体の機能が障害されるのではないかと予想されている[32]。

4．常染色体劣性型の DKC

常染色体劣性遺伝型の DKC の頻度は少なく，全体の１～２%にしか認められない[7]。これまでに原因遺伝子としては，前述の *TERT* や snoRNA である *NOP10*，*NHP2* が同定されている（表1）[7, 14]。常染色体劣性遺伝型の DKC に認められた *TERT* の変異は，RT ドメインの中に位置する R811C と R901W のホモ変異である[25]。これら

の変異の機能はhaploinsufficiency効果でテロメラーゼ活性を減弱させるが，ホモ変異であるためテロメラーゼ活性の減弱が強く，DKCやHHSの表現型を示す。しかし，これらの*TERT*変異のDKC発症形式が常染色体劣性遺伝型かは不明瞭で，R811C症例のヘテロの変異を有する両親は軽度ではあるがDKCの表現型とも考えられる症候を有しており，世代促進が進んでいないためにDKCの表現型が出ていないだけかもしれない。

NOP10やNHP2は，Dyskerinなどとsno RNA複合体を形成し，*TERC*のboxH/ACAドメインと結合し，テロメラーゼ複合体のprocessingと安定化の役割を果たしている[14, 20]。これまでに*NOP10*はホモ変異が，*NHP2*はホモ変異と両アレル変異が認められているが，これらの変異によって*TERC*の発現が減少し，テロメラーゼ活性が減弱することでDKCが発症すると考えられている[33, 34]。

近年，既知の原因遺伝子に変異を認めないDKC 2症例において，テロメラーゼ複合体のホロ酵素である*TCAB1*に両アレルの遺伝子変異が発見された[10]。*TCAB1*は*TERC*とCAB boxを介して結合し核内のCajalbodyに移行させ，Dyskerinや他のscaRNAsをCajalbodyに集積させることでテロメラーゼ複合体のprocessingを進める機能があると考えられている。この*TCAB1*のヘテロ変異を有する家族がDKCの表現型を示していないことや，*in vitro*での機能解析結果から，*TCAB1*は常染色体劣性型のDKCの原因遺伝子と考えられている[10]。

5．不全型のDKC

成人になって特徴的身体所見を伴わず緩徐に発症する，不全型のDKCの存在が明らかになった[35]。不全型のDKCは，臨床的には再生不良性貧血や骨髄異形成症候群などと診断されていることが多く[36, 37]，本邦においても再生不良性貧血や骨髄異形成症候群の不応性貧血などの骨髄不全症の2～5%に不全型のDKCが認められる[38～40]。不全型のDKCの原因遺伝子としては，*TERC*，*TERT*，*TINF2*の報告があるが，前述のように*TERC*，*TERT*の変異はhaploinsufficiency効果を示し，テロメラーゼ活性の減弱の程度は弱いため，DKCの表現型となるには世代促進や加齢が必要となることがある。こうした変異の場合は，世代の早い症例ではDKCの表現型が軽度で，不全型DKCとして診断されるのではないかと予想する（**図3**）。

これまでは再生不良性貧血の約1/3の症例はテロメア長が短縮し，再生不良性貧血の重症度，免疫抑制療法への不応性との関連が示唆されていたが[41～43]，これらは不全型DKCの存在が明らかになる以前の検討で，再生不良性貧血とテロメア長の短縮化が再生不良性貧血の病態にどのように関与しているかは明らかではない。しかし不全型のDKCは，効果の得られない免疫抑制療法が行われたり，血縁間同種造血幹細胞移植の際に健常人と区別が困難な軽症の不全型DKC同胞がドナーとして選ばれたりすることがあるため，臨床的に診断を明確にすることは大変重要である[35～40]。こうした不全型のDKCをスクリーニングするのに，骨髄不全症の診断時にテロメア長の測定をすることは有用であると考える。

6．早老症とテロメア

早老症はウェルナー症候群（**WS**：Werner Syndrome）やハッチンソン・ギルフォード・プロジェリア症候群（**HGPS**：Hutchinson-Gilford Proge-

WS (Werner Syndrome；ウェルナー症候群)
HGPS (Hutchinson-Gilford Progeria Syndrome；ハッチンソン・ギルフォード・プロジェリア症候群)

ria Syndrome）に代表される加齢促進状態をもたらす遺伝性疾患である[44]。臨床症状としては，若年時より皮膚の萎縮や骨粗しょう症などの通常の加齢現象が出現し，心血管障害や悪性腫瘍の発生が高率に認められる。

近年，早老症の一つと考えられているロスモンド・トムソン症候群（RTS：Rothmund Thomson Syndrome）や，poikiloderma with neutropenia（PN）の原因遺伝子の一つである *C16orf57* の変異が臨床的にDKCと診断された症例で発見された[45]。RTSやPNは，DKCと共通する特徴的身体的所見を多く認めることから，これらの疾患がオーバーラップするような症例の存在が示唆されている。しかし，*C16orf57* の変異を認めたDKC症例は，末梢血テロメア長の短縮が認められていない。このことは，従来のテロメア長短縮化によって発症するDKCとは異なる発症機序のDKCの存在を示唆している。

また，WSの原因遺伝子である *WS* 遺伝子や，HGPSの原因遺伝子である *LMNA* 遺伝子には，テロメア長を制御する機能がある。WSやHGPSでは皮膚や筋肉のテロメア長の短縮化を認めるが，血球系では *WS* 遺伝子や *LMNA* 遺伝子の発現がないため，テロメア長の短縮化は認められない[46, 47]。このことは，血液系，皮膚，毛根，筋肉など，それぞれ分化した細胞には特有のテロメア制御機構が存在することを示唆している。もしかしたら，前述の不全型DKCは，血球系のテロメア制御にのみ関与する未知の機序の存在を示唆しているかもしれない。

7．DKCの治療

現在のところ，DKCの根本的治療は開発されていない。DKCの主な死因は，造血障害に伴う様々な合併症と，晩期の悪性腫瘍によるものが大多数である[7, 12]。これまで前者に対しては造血幹細胞移植（stem cell transplantation：SCT）が試みられてきたが，通常の骨髄破壊的前処置によるSCTは，移植後の肺線維症などの肺合併症，消化管狭窄，肝中心静脈閉塞症などの治療関連毒性が強く，長期生存例は稀であった[48]。DKCにおいてSCTの治療関連毒性が強い理由は，皮膚，消化管，肺胞上皮などの幹細胞のテロメア伸長補正の障害による増殖障害があるためと予想されている[48]。その後，fludarabineをベースとした骨髄非破壊的前処置によるSCTでは，前述の治療関連毒性が軽減され，長期の生存例も認められるようになった[48～50]。しかし，前述のようにDKCはHHSから不全型のDKCまでその表現型は様々で，どのような症例に対してどの時期にどのようにしてSCTを行うかといった臨床的な適応は明らかになっていない。また，他の後天的な骨髄不全症に対するSCTに比べて，DKCに対してのSCTは晩期の悪性腫瘍の合併がより高率となる可能性もあり，今後の症例の蓄積が必要である。

DKCの骨髄不全症に対しての保存的治療として，以前よりanabolic steroidやG-CSFなどの有効性が報告されてきた[7, 51, 52]。特に，anabolic steroidであるoxymetholone（0.5～5 mg/kg/day）の治療によって，約2/3の症例で血液学的な何らかの有効性が認められたとされている。これまでanabolic steroidによるDKCの血液学的な改善の機序は不明であったが，近年，*TERT* のpromoter領域にエストロゲン結合領域が認められ，アンドロゲンやエストロゲンなどの性ホルモンがテロメラーゼ活性を亢進させることが示された[53]。このことから，成人以降で診断された不全型のDKCに対しても，anabolic steroidなどによる治療は有効であると思われる。

RTS（Rothmund Thomson Syndrome；ロスモンド・トムソン症候群）　PN（poikiloderma with neutropenia）
SCT（stem cell transplantation；造血幹細胞移植）　iPS（induced pluripotent stem）